

# Gas compositional effects on $CO_2$ Sequestration

## 1 Introduction

Controlling anthropogenic carbon dioxide ( $CO_2$ ) emissions is important due to the unequivocal evidence of the connection between global temperature increase and the increase in atmospheric  $CO_2$  concentrations. Geological sequestration of  $CO_2$  seems to provide an answer to this problem, where  $CO_2$  is concentrated and pumped into deep saline aquifers, coal formations or depleted oil reservoirs.[1]

## 2 Literature Review

Carbon dioxide sequestration can be defined as the capture and storage of  $CO_2$  that would have otherwise been emitted into the atmosphere by capturing and delivering it to secure storage[2].  $CO_2$  is sequestered geologically by three mechanisms:

1. Stratigraphic or structural trapping which is analogous to hydrocarbon capture in petroleum reservoirs, where  $CO_2$  is trapped as a supercritical phase
2. Hydrodynamic trapping through dissolution of  $CO_2$  into formation water
3. Mineral precipitation of carbonate phases such as calcite and magnesite

### 2.1 Fate of $CO_2$ underground

Once  $CO_2$  is injected into the storage media i.e., during the early stages of storage, physical trapping is likely to be the important trapping mechanism. Over time,  $CO_2$  will dissolve into the formation water at a rate

controlled by several factors such as the rate of  $CO_2$  injection, the rate of  $CO_2$  dissolution into the pore water, the surface area available for the reaction and the rate of diffusion of the  $CO_2$  into the pore water away from the pore water- $CO_2$  interface. But eventually mineral trapping which involves the formation of carbonate minerals, will make significant contributions to the long term sequestration of  $CO_2$ [3]. Hence broadly speaking, mineral precipitation can also be referred to as sequestration whereas physical trapping and hydrodynamic trapping can be termed as storage[4].

The carbon repository (geologic formations where  $CO_2$  is pumped into) is a complex structural and stratigraphic package containing diverse geochemical environments, brine and ground water, sandstone and rock compositions etc. The stability of the overlying confining bed should also be considered as it is critical for long-time containment of  $CO_2$ . Significant research and large-scale demonstrations are required to certify this method (pumping  $CO_2$  into geological formations) as safe, reliable and economically viable solution for  $CO_2$  sequestration.

## 2.2 Experimental work on Mineralogical Changes

Not much attention has been paid to the mechanisms that adversely impact the integrity of a carbon repository. Some simple numerical models (using Darcy equation and Fick's law) have been employed by Lindeberg et al. [5] to develop models which attributed the leakage of  $CO_2$  to gravity migration with subsequent release through sub vertical fractures and faults. Several numerical simulations were used to evaluate potential leakage by discharge through the confining rock or through a fracture or fault zone.

A few experimental studies examined geochemical reactions in a saline aquifer in response to  $CO_2$  injection. Gunter et al. [6] carried out numerical geochemical modeling studies that incorporated kinetic laws and some studies combining experiment and modeling, in which dissolution of silicate minerals in brine and precipitation of carbonate are reported. A major study in the identification of geochemical reactions within an experimental system at reservoir temperature and pressure was done by Kaszuba et al. (2003, 2005) [4, 7].

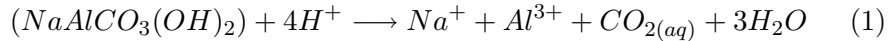
Kaszuba et al. (2003)[4] carried out a study to determine the extent of fluid rock interactions in addition to carbonate mineral precipitation that may occur in an experimental system that simulates geologic storage and sequestration of  $CO_2$ . Their reaction conditions were  $200^\circ C$  and  $2000\text{ psi}$ . The experimental setup used therein was a flexible cell hydrothermal apparatus with an Au-Ti (gold-titanium) reaction cell with a sampling port[8]. The

reactant mixture was arkose which consisted of quartz, oligoclase and microcline. Shale was used as an aquitard, the confining layer of the repository. The brine used was synthesized using laboratory grade salts to represent aquifer compositions in the Delaware basin. The brine + rock mixture was allowed to react for 59 days to achieve equilibrium and then  $CO_2$  was injected and then allowed to react for another 80 days. The solid phases were then analyzed using SEM (Scanning Electron Microscopy)/EDS (Energy Dispersive X-ray Spectroscopy), XRD (X-Ray Diffraction) analysis and the brine chemistry was analyzed using ICP-MS (Inductively Coupled Plasma Mass Spectrometry) for cations and Ion Chromatography for anions. The results observed were indicative of the geochemical reactions taking place in the repository. Clear euhedral crystals of magnesite were evident in the post reaction sample when analyzed through SEM. Siderite was seen growing on the shale surface. Microcline surface was seen to undergo severe etching. Patchy crystals of halite were present. Analcime crystals were found in abundance in the experiment. The brine chemistry also changed significantly after the experiments. The concentration of Na and Cl ions decreased initially but stabilized thereafter and were constant throughout. The concentration of all the trace ions Ca, Mg, Br, Fe, and  $SO_4$  all increased during the reactions. This indicated that all the minerals in the starting materials underwent significant changes mainly via dissolution, thus displaying evidence of participation in fluid rock reactions.

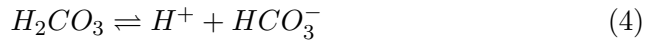
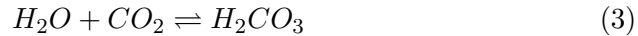
Kaszuba et al. (2005)[7] then carried out a study to analyze the effect of  $CO_2$  injection on fluid rock reactions. For this study they used the same experimental apparatus and starting materials as in their previous study. One experiment was with brine + rock without  $CO_2$  injection and the other experiment with  $CO_2$  injection and the changes in both the experiments were analyzed using the same techniques as their previous study. In the brine rock experiment the  $Na^+$  concentration initially decreases then increases and continues to decrease through out the experiment. The  $Cl^-$  concentration decreases then increases and remains stable for rest of the experiment. The pH decreased and then achieved a stable value. All the trace ions increased in their concentrations. In the experiment with  $CO_2$  injection the concentrations of  $Na^+$ ,  $Cl^-$  and the trace elements were similar to that of the brine rock experiment. The exception was Mg whose concentration was 3 to 10 times larger than the brine rock experiment. The pH was less for obvious reasons. No carbonate precipitation was observed in the brine-rock experiment but in the  $CO_2$ -brine-rock experiment two types of carbonate precipitations were observed. Magnesite occurs as large, discrete bladed crystal visible to the naked eye. Siderite occurs as euhedral crystal

on the shale indicating that the aquitard also is a reactive component of the carbon repository. So shale reactivity may produce an increase in porosity and permeability which increases the potential for the release of  $CO_2$ .

Precipitation of the mixed hydroxyl carbonates mineral dawsonite, predicted as a stable carbonate phase in the reactive transport models of carbon sequestration (Johnson et al. [9]; Knauss et al. 2002[10]) is not observed in any of the experimental studies. In the field large volumes of dawsonite were observed in oil shales in the Green river formations, but they are linked to highly alkaline solutions. A study of the stability of dawsonite was done by Hellevang et al. [11]. They concluded that dawsonite will become unstable as  $CO_2$  pressures decrease following injection. They measured dissolution rates of dawsonite at  $80^\circ C$  as a function of pH from 3 to 10. Use of these dissolution rates in reactive transport calculations indicate that dawsonite rapidly dissolves following the decrease of  $CO_2$  pressure out of its stability leading to the precipitation of kaolinite. They described the dawsonite dissolution using the reaction



Thus the stability of dawsonite can be attributed to aqueous  $CO_2$  concentrations which itself can be related to partial pressure of coexisting  $CO_2$  phase by



The relative stability of dawsonite with respect to other Na and Al bearing phases can be assessed using logarithmic activity fugacity diagrams which suggest that dawsonite stability increases with increasing  $\frac{a_{Na^+}}{a_{H^+}}$  and fugacity of  $CO_2$  but decreases with increasing temperature. Hence at higher temperatures higher  $CO_2$  fugacities are required to stabilize dawsonite. So following  $CO_2$  injection, as injected  $CO_2$  disperses, dissolves or leaks,  $CO_2$  fugacity would decrease, potentially destabilizing dawsonite to other alumino-silicate phases like kaolinite or albite.

When  $CO_2$  dissolves in water, pH decreases due to the formation of carbonic acid. Carbonate ion is provided by inducing calcite minerals or natural dissolution of calcite in the low pH state. Geological abundance

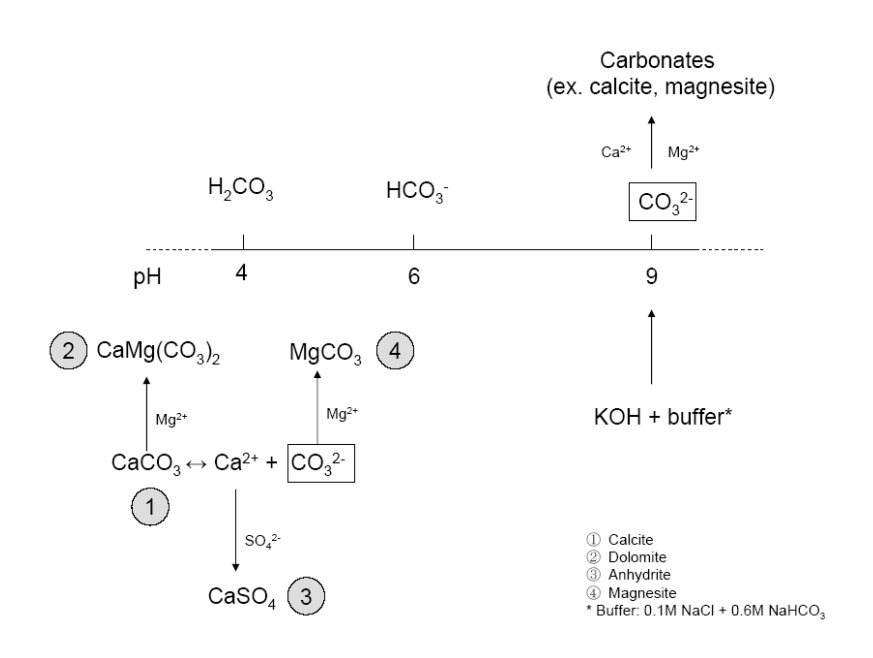
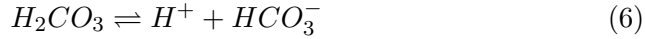


Figure 1: Dominant phase of carbonic acid with respect to solution pH.

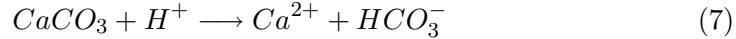
of magnesium minerals leads the process by maintaining a high pH in the aqueous phase by inducing KOH with buffer solution. Formation of carbonate minerals using simple pathways is shown in Figure 1.

Soong et al. [12] reported the dominant state of carbonic acid with respect to solution pH. The production of  $H_2CO_3$  dominates at a low pH of 4,  $HCO_3^-$  at a mid pH of 6 and  $CO_3^{2-}$  at a high pH of 9. In terms of carbonate formation, high pH of 9 is advantageous by the dominance of carbonate ion. Geologic abundance of cations in the aqueous phase may lead to the mineral sequestration.

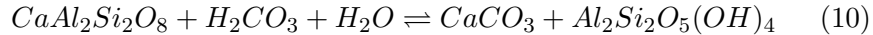
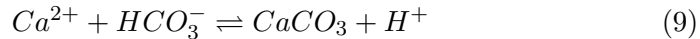
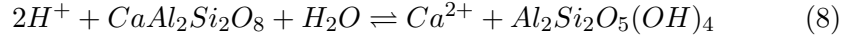
Rosenbauer et al. [13] presented the capacity for brine disposal with  $CO_2$  removal. They reported that this is possible due to scaling and a variation of porosity when  $CO_2$  is injected into a deep aquifer. They also showed that more  $CO_2$  may be trapped in a deep saline aquifer by the formation of bicarbonate ion ( $HCO_3^-$ ). They provided an insight into  $CO_2$  permanent sequestration by the dissolution and the formation of mineral carbonates



The sequential reactions result in decreasing pH value. Dissociated hydrogen ion can dissolve calcite, mainly  $CaCO_3$ , to produce calcium ion and bicarbonate



The generation of bicarbonate will lead to additional  $CO_2$  dissolution into the aqueous phase. Precipitation reactions can be also expected in the aqueous  $CO_2$  phase. For instance, arkosic sandstone as a carbonate reacts with hydrogen ion to precipitate calcium carbonate.



From two different scenarios (carbonate dissolution and precipitation) above, we can recognize that reactions of supercritical  $CO_2$ , aqueous  $CO_2$ , brine and rocks vary with their compositional differences, apart from temperature and pressure variance. Dissolution and precipitation of carbonates are simultaneously expected in complex rock environments. Therefore we

Brine	Co-Injected minerals	Porosity	Observation
Low-Sulphate	Limestone	+2.6%	–
High-Sulphate	Limestone	-4.9%	Precipitation of anhydrite and dolomitization of lime stone

Table 1: Porosity changes in  $CO_2$ -brine-rock system

Minerals	Solubility	Temperature	Pressure(bar)
Limestone	+9%	25°C	200
	+6%	120°C	200
Arkosic sandstone	+5%	120°C	300

Table 2: Solubility changes of  $CO_2$  in brine

need to consider the net porosity changes caused by dissolution and precipitation reactions in host rock environment.

Other reactions such as sulfate formation and ion exchange by magnesium ion are presented. Eqn (13) shows the conversion from calcite to dolomite.

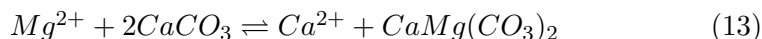
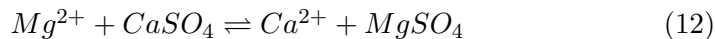
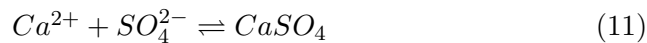


Table 1 and 2 summarize the result by Rosenbauer et al. (2005)[13]. Their experiments were carried out at 25°C and 120°C and 100 – 600 bar using 100-200 mesh size minerals. Brine with high sulfate ion generates the precipitation of anhydrite ( $CaSO_4$ ) and the dolomitization of limestone by aqueous  $CO_2$ , which decreases the net porosity. Participating in the formation of carbonates resulted in increase of  $CO_2$  solubility of up to 9 %.

The experiments reacting high sulfate brine with limestone, both in presence and absence of supercritical  $CO_2$  were characterized by the precipitation of anhydrite, dolomitization of limestone and a final decrease in porosity of 4.5%. The concentration of the ions in the liquid phase, in the experiments with PVB showed a similar trend to that of the results showed by Kaszuba et al[7] except that the concentrations of the ions were much less which may probably be due to the low temperature used in these experiments.

Drunckenmiller and Maroto-Valer [14] reported the importance of pH to form carbonates. Carbonic species exist in three different dominant phases

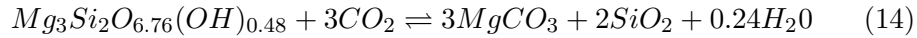
with respect to pH values. The production of  $H_2CO_3$  dominates at a low pH ( 4),  $HCO_3^-$  at a mid pH ( 6) and  $CO_3^{2-}$  at a high pH (9). This informs us that maintaining pH with the basic phase would be advantageous to precipitate carbonates. The main parameters affecting the carbonate precipitation/dissolution process are

1. Temperature
2. Pressure
3. Brine composition
4. Rock composition
5. pH

Temperature has greater influence on carbonate formation than pressure (increase in temperature increases the formation of carbonates). The trend of the fluid chemistry is similar to what was reported by Kaszuba et al. [7].

Nevertheless, it has been often cited that the slow reaction rate of mineral carbonates is disadvantageous for sequestration. Magnesium rich minerals may be viable to carbonation-base sequestration. For enhancing the reaction rate, Maroto-Valer et al. [14] suggested the activation of magnesium rich minerals (serpentine). They presented how to increase pore volume of magnesium rich minerals using physical and chemical treatments. Major cost for mineral activation is the heating process to remove surface hydroxyl groups. Chemical treatment using sulfuric acid results in high porosity of mineral with less magnesium in the surface. Geological abundance of magnesium minerals provides incentive for the study of carbonate sequestration.

Wolf et al. [15] developed the micro reaction ( $0.1 \text{ cm}^3$ ) system to observe in-situ reactions relevant to  $CO_2$  sequestration. They characterized the carbonation reaction using synchrotron X-ray diffraction and Raman spectroscopy. The objective of their micro reactor built with moissanite windows is to understand the carbonation reaction, which will provide cost effective process design.



Wellman and coworkers (2003) [16] suggested the permeability to porosity correlation

$$k = k_0 \left( \left( \frac{\phi}{\phi_0} \right) \right)^x \quad (15)$$

Minerals	Reaction rate constant ( $molcm^{-2}sec^{-1}$ )
Calcite	$1 * 10^{-5}$
Dolomite	$1 * 10^{-7}$
Magnesite	$1 * 10^{-7}$
Anhydrite	$1 * 10^{-6}$
Halite	$1 * 10^{-4}$
Quartz	$1 * 10^{-13}$

Table 3: Kinetic reaction rate constants as in Wellman et al[16].

$k$  and  $k_0$  are system and initial permeabilities,  $\phi$  and  $\phi_0$  are system and initial porosity, respectively.  $x$  is fitting constant and they chose a value of 3.4 for their experiments.

### 2.3 Core Flooding experiments

Izgec et al. [17] performed  $CO_2$  core flooding experiments and observed changes in the permeability and porosity of the core samples using computerized tomography (CT) monitored laboratory experiments.  $CO_2$  displacement in the core depends mainly on the following parameters:

1. multiphase flow characteristics
2. solution dissolution kinetics
3. solute transport
4.  $CO_2$  upward movement
5. hydrodynamic instabilities due to the displacement of brine with less viscous  $CO_2$

When  $CO_2$  is injected it dissolves in water, minerals such as calcite dissolve readily increasing porosity and permeability leading to increased flow rate and increased dissolution forming wormholes in the core. This process of dissolution and deposition process are characterized by the dimensionless numbers, Peclet (Pe) and Damkohler (Da). The effect of these two dimensionless parameters is shown in the Table 4.

Experiments were carried out using sandstone cores and  $CO_2$  saturated brine and characterization was done using X-ray CT scanner at a temperature of  $18^\circ C$  and a pressure of 500 *psi*. The composition of brine did not

Da large ( $Da \gg 1$ )	Rapid chemical reaction
Da small ( $Da \ll 1$ )	Slow chemical reaction
Pe large and PeDa large	Wormholes are formed
Pe small and PeDa large	Reactions mainly occur at inlet boundary resulting in near inlet dissolution
At moderate Pe and PeDa numbers	Reactions are generally non-uniform with more in the upstream and less in downstream

Table 4: Effect of the two dimensionless parameters Pe and Da on Dissolution and precipitation processes.

seem to affect the porosity and the permeability changes. The injection rate followed the same trend as predicted by the dimensionless numbers (Pe) and (Da). The effect of the flow direction (orientation of the core) plays a crucial role on rock property trends. For vertically oriented plugs the permeability increased and then decreased after a certain pore volume. On the other hand for the horizontally oriented core plugs the permeability initially decreased and then after a certain injection period stabilized. Porosity also showed the same trend. The difference may be due to the manner in which precipitated minerals block pore throats.

Krunhansl et al. [18] performed both  $CO_2$  core flooding and long term static tests and made an attempt to validate their modeling results (carried out with TOUGH REACT). For the core-brine experiments, characterization was done using SEM analysis. Both the core and the static tests were carried out at 700 *psi* and 40°C. The lithology of the sample consisted of fine grained arkosic sandstone with occasional petroleum stains. The main minerals identified were quartz, potassium feldspar and dolomite. The brine chosen was collected from the West Pearl Queen reservoir.

In the flow tests a relatively large (50%) decrease was noted, but no notable change in porosity was found. The reason for this decrease was not explained. In the static tests the post test fluid was captured and analyzed for cation by DCP and anions by IC. The dominant change was increase in salt content by 20%. The solids were analyzed using SEM which showed etching of the carbonate grains. There was fur growing on the margins of some grains which was insoluble in water.

Egermann et al. [19] performed similar core flooding experiments but at higher pressure of 100 *bar* and 90°C. The porosity measurements were done

by the NMR technique. The effect of flow rate was analyzed by varying the flow rate of  $CO_2$  saturated brine in the range of  $2cm^3/hr$  to  $500cm^3/hr$ . The results indicated that high flow rates favor worm hole dissolution patterns whereas low flow rates drive to compact dissolution patterns. The lateral extension of the wormholes seemed to be favored when sulfates had been removed from the brine. In the analysis of the test fluid,  $Ca^{2+}$  concentration increased continuously which could be directly related to the calcite dissolution. The concentration of  $SO_4^{2-}$  decreased continuously.

Similar core experiments were performed by Bateman et al. [3] and Wellmann et al. [16] who investigated the changes in the porosity and permeability and the effect of the brine composition, orientation of core and the injection rate on the reactions and thus the porosity and permeability of the core. The results were similar to those of Egermann et al. [19] and Krunhansl et al. [18].

## 2.4 Kinetics of Geochemical Reactions

Kinetics of geochemical reactions have been investigated over a long period of time. The reaction rates of different minerals such as kaolinite, dolomite, calcite, quartz, chlorite etc and the effect of pH temperature and pressure have been reported in the literature.

Carroll et al. [20] measured the dissolution rates,  $k_r$  of the mineral kaolinite at  $25^\circ C$ ,  $60^\circ C$  and  $80^\circ C$  which were highly dependant on pH. The experiments were conducted by placing kaolinite into polypropylene reaction vessels which were filled with 500 ml of different pH buffer solution to conduct the experiments at various pH. The solutions were analyzed for aluminum and silicon with a DCP emission spectrometer.

At all three temperatures,  $k_r$  decreases from acid to near neutral pH and increases from near neutral to alkaline pH. The pH dependency of kaolinite dissolution is attributed to the net adsorption of  $H^+$  and  $OH^-$  ions to aluminum and silicon reaction sites as well as to the formation of positively, neutral and negatively charged alumino-silicate complexes at acid, neutral and alkaline pH respectively. The diffusion of the elements through an amorphous surface layer also affects the overall rate of dissolution. The activation energies of the reactions were also calculated because the dissolution rate behavior was a function of temperature (and solution pH). The reactions at the mineral-solution interface were also explained using transition state theory and surface-complex reaction theory. The temperature dependence of kaolinite dissolution was described using the classical Arrhenius equation and the activation energies of the reaction at different pH were calculated

and compared with those already published in the literature.

Alkattan et al. [1] reported the dissolution rates of calcite and limestone as a function of pH from -1 to 3 and temperature from  $25^{\circ}C$  to  $80^{\circ}C$ . The dissolution rates were measured using the rotating disk technique (proposed by D.P Gregory and Riddiford 1956 [21]), which employed a double glass walled rotating disk reactor. Rates were determined from the weight loss of the solid samples dissolved in HCL solutions. Three types of samples were considered: single calcite crystals, limestones and compressed calcite powders. Two different limestones were also used.

The dissolution rates listed were calculated from

$$r = \frac{\Delta m}{stW} \quad (16)$$

Where  $\Delta m$  represents the weight loss of the solid,  $s$  designates the geometric surface area of the disk,  $t$  represents the elapsed time and  $W$  signifies the molecular weight of calcite ( $100.1g/mol$ ). The transport rate constant for the rotating disk reactor at disk rotation speeds  $\gg 0$  is given by Gregory et al. [21], Pleskov et al. [22], Alkattan et al. [1].

$$k_t = D/\delta = 0.62D^{2/3}\nu^{-1/6}\omega^{1/2} \quad (17)$$

$D$  stands for  $H^+$  diffusion coefficient,  $\delta$  signifies the thickness of the diffusion layer,  $\nu$  corresponds to the kinematic viscosity of solution and  $\omega$  represents the disk rotation speed. So for calcite dissolution from theory and the above equation it follows that for a rotating disk reactor

$$\frac{1}{r} = \frac{1}{k_2c_{H^+}\gamma_{H^+}} + \frac{1}{0.62D^{2/3}\nu^{-1/6}c_{H^+}}\omega^{-1/2} \quad (18)$$

Where  $r$  is the overall dissolution rate and is a linear function of the reciprocal of the square root of the rotating disk speed  $\omega^{-1/2}$ . The intercept of this straight line can be used to deduce  $k_2$ , the chemical rate constant while its slope allows determination of the diffusion coefficient  $D$ . The variation of  $H^+$  diffusion coefficients can be described with an Arrhenius equation and thus the activation energies and the pre-exponential factor are determined. The apparent rate constants and the  $H^+$  diffusion coefficients increase substantially with increasing temperature and are consistent with the corresponding values published in the literature.

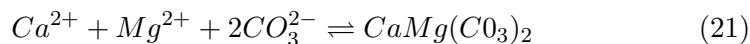
Arvidson and Mackenzie [23] measured the rate of precipitation of dolomite and its dependence on temperature and solution composition. They quantified and modeled kinetics by the application of a rate law that represents rate as a simple function of saturation index (as stated by Lasaga [24])

$$r = k(\Omega - 1)^n \quad (19)$$

Where  $\Omega$  is the saturation index of the solution with respect to ideal dolomite given by

$$\Omega = \frac{a_{Ca^{2+}}a_{Mg^{2+}}a_{CO_3^{2-}}}{K_{T,Dol}} \quad (20)$$

This law was tested using a series of experiments by measuring the steady state rate of dolomite precipitation in a dolomite seeded flow reactor. The dependence of the kinetics on the fluid composition was determined by varying the saturation index from near saturation to 100. The temperature was also varied from  $100^\circ C$  to  $200^\circ C$  to solve for the reaction order and the Arrhenius rate constant  $k = A \exp(\frac{-\epsilon_a}{RT})$  of this rate law. The experiments were conducted in a steady state plug flow reactor with recycle. The reactor was filled with a  $> 2\mu$  m pore size (5g) dolomite seed material. The pressure was maintained at 100 *psi* by a back pressure regulator. The overall precipitation reaction proceeds as



Selective fitting of rate data gives values for activation energy  $\epsilon_A$ , pre-exponential frequency factor A and reaction order n of 31.9 *Kcal/mol*, 101.05 and 2.26 respectively. The comparison of values for activation energy with those computed from other sources and with those estimated from thorough consideration of heats of cation hydration suggests that  $Mg^{2+}$  dehydration represents a significant component of  $\epsilon_A$ , the activation energy associated with cation ordering. The style of growth of the dolomite crystals varies according to the extent of super saturation, with lower value promoting simple migration of surface steps and kinks. Higher saturations are associated with the development of complex nucleation centers consisting of sub-micron sized nuclei. The effective dolomite precipitation rate is maximized in the absence of other carbonate phases like calcite. Thus one can conclude that the overall rate of dolomite precipitation relative to the competing carbonate phases at surface temperatures determines the abundance of dolomite in a sedimentary regime.

Gautelier et al. [25] measured the rate of dolomite dissolution as a function of pH from -0.5 to 5 and temperature from  $25^\circ C$  to  $80^\circ C$ . Same experimental method as used by Alkattan et al. [1] (to measure the dissolution rates of calcite) was employed here. The use of rotating disk techniques and

the comparison of the experimental data to the equations reported by Gregory and Riddiford [21] yielded steady state dissolution rates as a function of the solution pH adjacent to the dolomite surface. Rates at all temperatures and for  $1 < pH < 5$  were found to be consistent with the rate law

$$r = k_1 a_{H^+}^n \quad (22)$$

Where  $r$  refers to surface area normalized dissolution rate,  $k_1$  is the reaction rate constant and  $a_{H^+}$  refers to hydrogen ion activity in the solution.

The variation of dolomite dissolution rates with temperature were described in terms of an Arrhenius equation in the form  $r = A \exp(\frac{-E_a}{RT})$ . The apparent activation energy decreases dramatically with pH from  $46 KJ/mol$  at  $pH = 0$  to  $15 KJ/mol$  at  $pH=5$ . The overall dissolution process was found to be surface reaction limited at  $pH < 1$ , but the effect of diffusional transport becomes increasingly significant with increasing pH.

Gautelier et al. [25] studied dolomite dissolution rates at  $80^\circ C$  as a function of chemical affinity and solution composition. They used the dissolution mechanism proposed by Pokrovsky et al. [26] where the rates are controlled by the detachment of the  $Mg(OH)_2^+$  species at the dolomite surface. The dolomite dissolution rates were described using the expression

$$r = k_{Mg^+} \left[ \frac{K_{CO_3^*} K_{Ca^*}}{K_{CO_3^*} K_{Ca^*} + K_{Ca^*} a_{CO_3^{2-}} + a_{CO_3^{2-}} a_{Ca^{2+}}} \right]^n (1 - \exp(-n_A/RT)) \quad (23)$$

$k_{Mg^+}$  Designates rate constant

$K_{CO_3^*}, K_{Ca^*}$  Denote equilibrium constants

$a_i$  refers to activity of subscripted aqueous species

$A$  is the chemical affinity of the dissolving dolomite

$n$  denotes the stoichiometric coefficient

Rates were calculated from the difference between the inlet and outlet solution calcium and magnesium concentrations. Ca and Mg were analyzed by atomic absorption spectrometry (AAS) or by complexometric titration with EDTA. The dolomite dissolution rates at  $80^\circ C$  in aqueous solution decreased with increased carbonate activity. The data are also found to be consistent with Pokrovsky and Schott [27] dolomite dissolution mechanism.

Liu et al. [28] did a comparative study on the dissolution rates of dolomite and limestone. For limestone under the condition of  $CO_2$  partial pressures  $> 100 Pa$  dissolution rates increased significantly by a factor of

about ten after addition of carbonic anhydrase (CA) into the solution which catalysed the conversion reaction of  $CO_2$  whereas CA had little influence on dolomite dissolution. Moreover the dissolution of limestone was more sensitive to hydrodynamics (rotation speed) than dolomite dissolution. Measurements of the dissolution rates were performed at a fixed rotating speed and concentration of CA by measuring the increase in conductivity. The increase in the dissolution rate by addition of CA for limestone and dolomite were highly sensitive. Both the carbonate rock dissolutions increased with increase in  $P_{CO_2}$ .

Pokrovsky et al. [29] measured the dissolution rates of calcite, dolomite and magnesite at  $25^\circ C$  and pH from 3 to 4 as a function of salinity and partial pressure of  $CO_2$ . Experiments on calcite and dolomite (both crystals and powders of  $100\text{-}200\mu\text{m}$ ) were conducted in a batch reactor under controlled hydrodynamic conditions using the rotating disk technique. The in situ pH was measured using a solid contact electrode in a cell without liquid junction. The results indicate that the carbonate mineral dissolution rates were proportional (weakly dependent) on  $P_{CO_2}$  but not  $H_2CO_3^*(aq)$ . For dolomite and magnesite the surface complexation model (SCM) of Pokrovsky et al. [26] [30] predicts dissolution rates up to  $50\text{ atm}$  with good accuracy.

## 2.5 Modeling Mineralogical Changes

Xu et al. [31] performed numerical simulations with the reactive fluid flow and geochemical transport code TOUGHREACT to analyze mass transfer between sandstone and shale layers and  $CO_2$  immobilization through mineral precipitation. Earlier work by Xu et al. [32][33] presented a geochemical modeling analysis of the interaction of aqueous solutions under high  $CO_2$  partial pressures with three different rock types. The first rock was glauconitic sandstone from the Alberta Sedimentary basin. The second rock type evaluated was a proxy for a sediment from the United States Gulf Coast. The third rock type was a dunite, an essentially monomineralic rock consisting of olivine.

Xu et al. [32] performed reactive transport simulations of a 1-D radial well region under  $CO_2$  injection conditions in order to analyze  $CO_2$  immobilization through carbonate precipitation, using Gulf Coast Sandstones of the Frio formation of Texas. Most of the simulated mineral alteration pattern was consistent with the observations while some inconsistencies were also observed. For example, quartz abundance declined over the course of simulation, while quartz overgrowths were observed during diagenesis due to the release of  $SiO_2$  during the replacement of smectite by illite in adjacent

shales [34].

Xu et al. [32][33] made many simplifications and approximations such as

1. treating the sandstone aquifer as if it were a closed system isolated from the enclosing shales
2. not adequately representing the extremely complex process of kerogen decomposition in deeply buried sediments

Xu et al. (2005) [31] carried out simulations using the non-isothermal reactive geochemical transport code TOUGHREACT [35]. A reactive geochemical transport model for a sandstone-shale system under high  $CO_2$  pressures was developed. The model was used to analyze the mass transfer of aqueous chemical components, the alteration pattern of minerals, sequestration of  $CO_2$  by secondary carbonates and changes of porosity in a Gulf Coast aquifer.

Andre et al. [36] presented numerical results performed by TOUGHREACT of two  $CO_2$  injection scenarios, first with  $CO_2$ -saturated water and second with pure supercritical  $CO_2$ . Simulations show high reactivity of  $CO_2$  saturated water with porosity increasing up to 90%, associated with strong carbonate dissolution, in qualitative agreement with wormholing observed in some experimental investigation [19]. The second scenario shows a much lesser geochemical activity. If the porosity increases by about 5% to 7% in most part of the reservoir then there is a decrease observed in the vicinity of the injector due to mineral precipitations.

Cipolli et al. [37] gathered geochemical data on spring waters through an extensive survey of the Gruppo di Voltri area and confirmed that progressive interaction between ultrafamic rocks variably affected by serpentinization and meteoric waters produces  $Mg-HCO_3$  waters first, in shallow aquifers open to  $CO_2$  exchange, followed by the development of  $Na-HCO_3$  and  $Ca-OH$  type waters, under closed system conditions with respect to  $CO_2$ . The reaction path modeling of high-pressure  $CO_2$  injection into deep serpentinitic aquifers appears to represent a feasible option to reduce anthropogenic  $CO_2$  inputs into the atmosphere as these aquifers have a high  $CO_2$  sequestration capacity, mainly through mineral fixation as magnesite and subordinately through solution trapping.

Gaus et al. [38] performed numerical simulations to model the impact of reactive transport on Clayey cap rock at Sleipner (North sea) because of  $CO_2$  injection. The simulations show that although initially some dissolution occurs, feldspar alteration is the dominant long term reaction whereby the

exact mineralogical composition of the plagioclase fraction in the cap rock plays a crucial role. Diffusion in the cap rock is a slow process and the section of the cap rock which is exposed to geochemical interactions due to  $CO_2$  injection is limited to the rock adjacent to the reservoir. These reactions can cause a slight decrease in porosity.

Knauss et al. [10] evaluated the impact of  $CO_2$ , co-contaminant gas, aqueous fluid and reservoir rock interactions on the geologic sequestration of  $CO_2$ . They simulated the results of  $CO_2$  and co-contaminants into a specific heterogeneous rock formation and calculated the mineralogical changes along the path by coupling a chemical model with a simplified fluid flow using the reactive transport code CRUNCH proposed by Steefel et al. [39]. They found that even relatively large amounts of co-injected  $H_2S$  should not prove problematic for a  $CO_2$  injection process. In the case of  $SO_2$ , if conditions allow the S to be oxidized, only minor amounts of this could be tolerated due to the extremely low pH generated. Potential porosity loss due to the formation of anhydrite will also need to be assessed.

Lagneau et al. [40] carried out a study on the coupled reactive transport modeling by simulating the chemical reactions likely to occur in the system coupled to reactive transport at large time and space scales. They used HYTEC, a reactive transport code initially developed for transport of chemical solutions and colloidal matter in column systems. They concluded that transport controlled the dispersion of the dissolved  $CO_2$  in the carbonated aquifer, with a quick dissolution of the whole supercritical  $CO_2$  bubble and a transport of all the injected  $CO_2$  bubble in the flow direction. In case of a sandstone aquifer, the evolution is controlled by the reactivity of the dissolved  $CO_2$  with the host rock minerals. They also concluded that despite the poor ionic solvent capacity of supercritical  $CO_2$ , its activity may not be negligible.

White et al. [41] simulated the reactive transport of injected  $CO_2$  on the Colorado Plateau in Utah. They investigated the injection of  $CO_2$  into non dome shaped geologic structures that do not provide the traps which are traditionally deemed necessary for the development of artificial  $CO_2$  reservoirs. They developed two Tough2/ChemTOUGH2 integrated finite difference models of the geology and ground water along the above mentioned geologic structures. They found that 1000 years after the 30 year injection period began approximately 21% of the injected  $CO_2$  was permanently sequestered as mineral, 52% was beneath the surface as gas or dissolved in the ground water and 17% had leaked to the surface and leakage to the surface was continuing.

Zerai et al. [42] conducted equilibrium, path of reaction and kinetic

modeling of  $CO_2$ -brine-mineral reactions in the Rose Run Sandstone, one of Ohio's deep saline aquifers to investigate the factors that are likely to influence the capacity of this formation to trap solid  $CO_2$  as solid carbonate mineral phases. Geochemist's work bench(GWB) version 3.2.2 was used for equilibrium, path of reaction and kinetic modeling of  $CO_2$ -brine-mineral reactions. They concluded that dissolution of albite, K-feldspar and galuconite and the precipitation of dawsonite and siderite are potentially very important for mineral trapping of  $CO_2$ . The stability of carbonate rocks is controlled by the brine to rock ratio, reactive surface area,  $f_{CO_2}$  and porosity.

Battistelli et al. [43] described an EOS( Equation of State) module to handle the three component mixtures of water, sodium chloride and a slightly soluble non-condensable gas.

Xu et al. (1999) [44] explained how to apply the sequential module to solve the multi-component reactive transport problem in Toughreact.

Nghiem et al. [45] described the governing equation and solution method of the simulator (GEM-GHG).

Kumar et al. [46], Xu et al. [47], Franklin et al. [48] gave detailed description of the storage of  $CO_2$  in deep saline aquifers.

Neal et al. [49], Saikat et al. [50], Siriwardane et al . [51] simulated the impact of  $CO_2$  injection into coal beds.

Yousef et al. [52], Jessen et al. [53], Shtepani et al. [54] conducted numerical simulations to evaluate the impact of  $CO_2$  injection into depleted oil reservoirs.

Xu et al.. (2003) [32], Ozah et al. [55] studied the impact of injection of other co-contaminant gases along with  $CO_2$ .

Spiteri et al. [56] examined the relative-permeability hysteresis, its importance and its application to Geological  $CO_2$  Sequestration.

Bryant et al. [57] discussed the importance of Buoyancy-Dominated Multiphase Flow and its impact on geological sequestration of  $CO_2$ .

## References

- [1] M. Alkattan, E. H. Oelkers, J.-L. Dandurand, and J. Schott, "An experimental study of calcite and limestone dissolution rates as a function of pH from -1 to 3 and temperature from 25°C to 80°C," *Chemical Geology*, pp. 199–214, 1998.
- [2] S. Bachu and J. Adams, "Sequestration in geological media in response to climate change: capacity of deep saline aquifers to sequester CO<sub>2</sub> in solution," *Energy conversion and management.*, vol. 44, pp. 3151–3175, 2003.
- [3] K. Bateman and G. Turner, "Large scale column experiment: Study of carbon dioxide, pore water, rock reactions and model test case," *Oil and Gas Technology*, vol. 60, pp. 161–175, 2006.
- [4] J. P. Kaszuba, D. R. Janecky, and M. G. Snow, "Carbon dioxide reaction processes in a model brine aquifer at 200°C and 200 bar: Implications for geologic sequestration of carbon," *Applied Geo-Chemistry*, vol. 18, pp. 1065–1080, 2003.
- [5] E. Lindeberg, "Escape of Carbon Dioxide from aquifers," *Energy conversion and management.*, vol. 38, pp. 238–240, 1997.
- [6] W. D. Gunter and E. H. Perkins, "Aquifer disposal of CO<sub>2</sub>-rich greenhouse gases: Extension of the time scale experiment for CO<sub>2</sub>-sequestering reactions by geo-chemical modeling," *Mineral. petrol.*, vol. 59, pp. 121–140, 1997.
- [7] J. P. Kaszuba, D. R. Janecky, and M. G. Snow, "Experimental evaluation of mixed fluid reactions between supercritical carbon dioxide and NaCl brine: Relevance to the integrity of a geologic carbon repository," *Chemical Geology*, vol. 217, p. 277–293, 2005.
- [8] Ulmer and Barnes, Eds., *Hydrothermal Experimental Techniques*. John Wiley and sons, NY, 1987.
- [9] J. W. Johnson, J. J. Nitao, C. I. Steefel, and K. G. Knauss, "Reactive transport modeling of geologic CO<sub>2</sub> sequestration in saline aquifers: The influence of intra-aquifer shales and the relative effectiveness of structural solubility and mineral trapping during prograde and retrograde sequestration." *Proc., Natl. Conf. Carb. Seq.*, 2001.

- [10] K. G. Knauss, J. W. Johnson, and C. I. Steefel, "Evaluation of the impact of Carbon Dioxide, co-contaminant gas, aqueous fluid and reservoir rock interactions on the geologic sequestration of Carbon Dioxide," *Chemical Geology*, vol. 217, pp. (339–350), 2005.
- [11] H. Hellevang, P. Aagaard, E. H. Oelkers, and B. Kvamme, "Can dawsonite permanently trap Carbon Dioxide?." *Environmental Science and Technology*, vol. 39, pp. 8281–8287, 2005.
- [12] Y. Soong, A. L. Goodman, S. W. Hedges, J. R. Jones, and D. K. Harrison, " $CO_2$  Sequestration and importance of pH," *Prepr. Pap.-Am. Chem. Soc., Div. Fuel Chem*, vol. 47, pp. 43–48, 2002.
- [13] R. J. Rosenbauer, T. Koksalan, and J. L. Palandri, "Experimental investigation of  $CO_2$  brine rock interactions at elevated temperature and pressure: Implications for  $CO_2$  sequestration in deep-saline aquifers." *Fuel Processing Technology*, vol. 86, pp. 1581–1597, 2005.
- [14] M. L. Druckenmiller, M. M. Maroto-Valer, and M. Hill, "Investigation of carbon sequestration via induced calcite formation in natural gas well brine," *Energy and Fuels*, 2005.
- [15] G. H. Wolf, A. V. G. Chizmeshya, J. Diefenbacher, and M. J. Mckelvy, "In situ observation of  $CO_2$  sequestration reactions using a novel micro-reaction system." *Environmental Science and Technology*, vol. 38, pp. 932–936, 2004.
- [16] T. P. R. B. Grigg and B. J. McPherson, "Evaluation of Carbon Dioxide-Brine-Reservoir rock interactions with laboratory flow tests and Reactive Transport modeling," in *Society of Petroleum Engineers 80228*, 2003.
- [17] O. Izgec, B. Demiral, H. Bertin, and S. Akin., " $CO_2$  injection into saline carbonate aquifer formations -laboratory investigation." *Transport in porous media*, 2003.
- [18] J. Krumhasl, R. Pawar, R. Grigg, H. Westrich, N. Warpinski, D. Zhang, N. Jove-Colon, P. Lichner, J. Lorenz, R. Svec, B. Stubbs, S. Cooper, C. Bradley, J. Rutledge, and C. B. ., "Geological sequestration of  $CO_2$  in a depleted oil reservoir," in *Society of Petroleum Engineers*, 2002.
- [19] P. Egermann, B. Bazin, and O. Vizika, "An experimental investigation of Reaction Transport phenomena during  $CO_2$  Injection," in *Society of Petroleum Engineers*, 2005.

- [20] S. A. Carroll and J. V. Walther, "Kaolinite dissolution at 25°C, 60°C and 80°C," *American Journal of Science*, vol. 290, pp. 797–810, 1990.
- [21] A. Gregory, D. Pand Riddiford, "Transport to the surface of a rotating disc," *Journal of Chemical Society, London*, vol. 3, pp. 3756–3764, 1956.
- [22] Y. Pleskov and V. Filinovski, *The Rotating Disc Electrode*. Consultant Bureau, NY, 1976.
- [23] R. S. Arvidson and F. T. Mackenzie, "The dolomite problem: Control of precipitation kinetics by temperature and saturation state," *American Journal of Science*, vol. 299., pp. 257–288, 1999.
- [24] A. Lasaga and R. J. Kirkpartick, *Reviews in Mineralogy - Kinetics of Geo-Chemical processes*, P. H. Ribbe, Ed. Mineralogical society of America, 1981.
- [25] M. Gautelier, E. H. Oelkers, and J. Schott, "An experimental study of dolomite dissolution rates as a function of pH from -0.5-5 and temperature from 25°C to 80°C." *Chemical Geology*, vol. 157, pp. 13–26, 1999.
- [26] O. Pokrovsky, J. Schott, and T. F., "Dolomite surface speciation and reactivity in aquatic systems," *Geochimica et Cosmochimica Acta*, vol. 63, pp. 3133–3143, 1999b.
- [27] O. Pokrovsky and J. Schott, "Kinetics and mechanism of Dolomite dissolution in neutral to alkaline solutions revisited," *American Journal of Science*, vol. 301, pp. 597–626, 2001.
- [28] Z. Liu, D. Yuan, and W. Dreybrodt, "Comparative study of dissolution rate-determining mechanisms of limestone and dolomite," *Environmental Geology*, vol. 49, pp. 274–279, 2005.
- [29] O. Pokrovsky, J. Schott, and S. V. Golubev, "Dissolution kinetics of calcite, dolomite and magnesite at 25°C and 0 to 50 atm of Carbon Dioxide pressure:," *Chemical Geology*, vol. 217, pp. 239–255, 2005.
- [30] O. Pokrovsky, J. Schott, and T. F., "Processes at the magnesium bearing carbonates/solution interface- A surface speciation model of magnesite." *Geochimica et Cosmochimica Acta*, vol. 63, pp. 863–880, 1999a.
- [31] T. Xu, J. A. Apps, and K. pruess, "Mineral Sequestration of carbon dioxide in a sandstone-shale system," *Chemical Geology*, vol. 217, pp. 295–318, 2005.

- [32] T. Xu, J. Apps, and K. Pruess, "Reactive geo-chemical transport simulation to study mineral trap for  $CO_2$  disposal in deep Arenaceous formations," *Geophysical research letters*, vol. B2, pp. 108–120, 2003.
- [33] T. Xu, J. A. Apps, and K. Pruess, "Numerical simulation to study mineral trapping for  $CO_2$  disposal in deep aquifers," *Applied Geo-Chemistry*, vol. 19, pp. 917–936, 2004.
- [34] L. L.S, "Frio sandstone diagenesis, Texas Gulf coast a regional isotopic study," *Clastic Diagenesis, AAG Memoir*, vol. 37, pp. 47–62, 1984.
- [35] K. Pruess, O. C, and M. G, "Tough2 users guide version 2," Lawrence Berkeley Laboratory Report, Tech. Rep., 1999.
- [36] L. Andre, M. P Audigane, and A. Menjoz, "Numerical Modeling of fluid-rock chemical interactions at the supercritical  $CO_2$ -liquid interface during  $CO_2$  injection into a carbonate reservoir , the Dogger aquifer (Paris Basin, France)," *Energy Conversion and Management*, vol. 217, pp. 385–410, 2007.
- [37] F. Cipolli, B. Gambardella, L. Marini, G. Ottonello, and M. V. Zuccolini, "Geo-chemistry of high pH waters from serpentinites of the Gruppo Di Voltri (Genova, Italy ) and reaction path modeling of  $CO_2$  sequestration in serpentinite aquifers," *Applied Geo-Chemistry*, vol. 19, pp. 787–802, 2004.
- [38] I. Gaus, M. Azaroual, and I. Czernichowski-Lauriol, "Reactive Transport modeling of the impact of  $CO_2$  injection on the clayey cap rock at Sleipner (North Sea)," *Chemical Geology*, vol. 217, pp. 319–337, 2005.
- [39] S. C. I, "Crunch," Lawrence Livermore National Laboratory, Tech. Rep., 2001.
- [40] V. Lagneau and A. P. anf H. Catalette, "Reactive Transport modeling of  $CO_2$  sequestration in deep saline aquifers," *Oil and Gas Science and Technology*, vol. 60, pp. 231–247, 2005.
- [41] S. White, R. Allis, J. Moore, T. Chidsey, C. Morgan, W. Gynn, and M. Adams, "Simulation of reactive transport of injected  $CO_2$  on the Colorado Plateau, Utah, USA," *Chemical Geology*, vol. 217, pp. 387–405, 2005.

- [42] B. Zerai, B. Z. Saylor, and G. Matisoff, "Computer simulation of  $CO_2$  trapped through mineral precipitation in the Rose Run Sandstone , Ohio," *Applied Geo-Chemistry*, vol. 21, pp. 223–240, 2006.
- [43] A. Battistelli, C. Calore, and K. Pruess., "The simulator Tough2 / EWASG for modeling geothermal reservoirs with brines and non-condensable gas," *Geothermics*, vol. 26, pp. 437–464, 1977.
- [44] T. Xu, S. J. A. C, M. M, and C. E, "Modeling of non-isothermal multi-component reactive transport in field-scale porous media flow system," *Journal of Hydrology*, vol. 214, pp. 144–164, 1999.
- [45] L. Nghiem, P. Sammon, J. Grabenstetter, and H. Ohkuma, "Modeling  $CO_2$  storage in aquifers with a fully coupled geochemical EOS compositional simulator," in *SPE 89474.*, 2003.
- [46] A. Kumar, R. Ozah, M. Noh, G. Pope, S. Bryant, K. Sepehrnoori, and L. Lake, "Reservoir simulation of  $CO_2$  storage in deep saline aquifers," in *SPE 89343.*, 2002.
- [47] T. Xu, J. A. Apps, and K. Pruess, "Geologic sequestration of  $CO_2$  and associated  $H_2S$  and  $SO_2$  in bedded sandstone-shale sequences," in *American Geophysical Union Fall Meeting*, 2003.
- [48] F. M and O. Jr, "Storage of carbon dioxide in geologic formations," in *SPE 88842*, 2001.
- [49] W. N. Sams, G. Bromhal, O. Odusote, S. Jikich, T. Ertekin, and D. H. Smith, "Simulating carbon dioxide sequestration/ECBM production in coal seams: Effects of coal properties and operational parameters," in *SPE 78691.*, 1999.
- [50] S. Mazumder, A. Karnik, and K. H. Wolf, "Swelling of coal in response to  $CO_2$  sequestration for ECBM and its effect on fracture permeability," in *SPE 97754*, 2001.
- [51] Siriwardane, D. Smith, F. Gorucu, and T. Ertekin, "Influence of shrinkage and swelling of coal on production of coalbed methane and sequestration of carbon dioxide," in *SPE 102767*, 2001.
- [52] Y. Ghomian, G. A. Pope, and K. Sepehrnoori, "Hysteresis and field-scale optimization of WAG injection for coupled  $CO_2$ -EOR and sequestration," in *SPE 110639*, 2000.

- [53] K. Jessen and E. Stenby, “Fluid characterization for miscible EOR projects and  $CO_2$  sequestration,” in *SPE 97192*, 2001.
- [54] E. Shtepani, “ $CO_2$  sequestration in depleted gas/condensate reservoirs,” in *SPE 102284*, 2004.
- [55] R. Ozah, S. Lakshminarasimhan, G. Pope, K. Sepehrnoori, and S. Bryant, “Numerical simulation of the storage of pure  $CO_2$  and  $CO_2$ - $H_2S$  gas mixtures in deep saline aquifers,” in *SPE 97255*, 2000.
- [56] E. Spiteri, R. Juanes, M. Blunt, I. Colledge, and F. O. Jr, “Relative-Permeability Hysteresis: Trapping Models and Application to Geological  $CO_2$  Sequestration,” in *SPE 96448*, 2001.
- [57] S. Bryant, S. Lakshminarasimhan, and G. Pope, “Buoyancy-Dominated Multiphase Flow and its impact on Geological Sequestration of Carbon Dioxide,” in *SPE 99938*, 2002.